1 Characterization of three new condensation particle counters for sub-3 nm particle detection during
2 Helsinki CPC workshop: ADI versatile water CPC, TSI 3777 nano enhancer and boosted TSI 3010

4 Juha Kangasluoma[1], Susanne Hering[2], David Picard[3], Greg Lewis[2], Joonas Enroth[1], Frans Korhonen[1],
5 Markku Kulmala[1], Karine Sellegri[3], Michel Attoui[1,4], Tuukka Petäjä[1]
6
7 [1] Department of Physics, P.O. Box 64, 00014, University of Helsinki, Helsinki, Finland
8 [2] Aerosol Dynamics Inc., Berkeley, CA, USA
9 [3] Laboratoire de Météorologie Physique, UMR6016, Observatoire de Physique du Globe de
10 Clermont-Ferrand, CNRS – Université Blaise Pascal, Clermont-Ferrand, France
11 [4] University Paris Est Creteil, University Paris-Diderot, LISA, UMR CNRS 7583, France

13 Abstract

15 In this study we characterized the performance of three new particle counters able to detect particles
16 smaller than 3 nm during Helsinki CPC workshop in summer 2016: Aerosol Dynamics Inc versatile
17 water condensation particle counter (v-WCPC, ADI, Berkeley, USA), TSI 3777 nano enhancer (TSI Inc.,
18 Shoreview, USA) and modified and boosted TSI 3010 type CPC from Clermont Ferrand University called
19 as B3010. The performance of all CPCs was first measured with charged tungsten oxide test particles
20 at temperature settings which resulted in supersaturation low enough to not detect any ions produced
21 by a radioactive source. Due to similar measured detection efficiencies, additional comparison
22 between the 3777 and v-WCPC were conducted using electrically neutral tungsten oxide test particles,
23 and with positively charged tetradodecylammonium bromide. Furthermore, the detection efficiencies
24 of the 3777 and v-WCPC were measured with boosted temperature settings yielding supersaturation
25 which was at the onset of homogeneous nucleation for the 3777, or confined within the range of liquid
26 water for the ADI v-WCPC. Finally, CPC specific tests were conducted to probe the response of the
27 3777 to various inlet flow relative humidities, of the B3010 to various inlet flow rates, and of the v-
28 WCPC to various particle concentrations. For the 3777 and v-WCPC the measured 50% detection
29 diameters (d50) were in the range of 1.3 – 2.4 nm for the tungsten oxide particles depending on the
30 particle charging state and CPC temperature settings, and between 2.5 and 3.3 nm for the organic test
31 aerosol, and 3.2 – 3.4 nm for tungsten oxide for the B3010.

32
33 1 Introduction
34
35 The work of Stolzenburg and McMurry (1991) started a new chapter in aerosol research with their
36 prototype laminar flow condensation particle counter (CPC) capable of detecting 3 nm aerosol
37 particles via condensation of butanol vapor. Compared to the previous CPC designs, the significant
38 improvements in the instrument included minimized diffusion losses in the sampling line and a sheath
39 flow in the condenser to focus the particle beam to the maximum butanol supersaturation region in
40 the middle of the condenser (Wilson et al., 1983). This instrument is the predecessor of the ultrafine
41 CPC 3025A and 3776 (TSI Inc., Shoreview, USA), which currently are widely used in various fields of
42 aerosol science to study particle dynamics at particle sizes larger than 3 nm (e.g. Weber et al., 1996;
43 Aalto et al., 2001).
44   It was not possible to detect particles smaller than 3 nm with the CPC technology until 1997,
45 when Seto et al. (1997) published their design on the particle size magnifier (PSM) used to study
46 heterogeneous nucleation of dibutyl phthalate vapor onto small ions. Their advances were made
47 possible by the development of a new differential mobility analyzer (DMA) combined to an
48 electrospray source, allowing the CPC testing with well-characterized monomobile samples. Their CPC
49 was based on the design of Okuyama et al. (1984), which is a mixing type CPC. It took until 2011 to
50 commercialize the diethylene glycol (DEG) based mixing type CPC technology, when Vanhanen et al.

51 (2011) published their version of the DEG based PSM, today sold as the Airmodus A10 PSM (A11 nano
52 condensation nuclei counter when combined to Airmodus A20 butanol CPC).

53 The first use of DEG as a CPC working fluid was reported by Iida et al. (2009), who studied
54 sub-3 nm particle detection via heterogeneous nucleation with many different working fluids
55 theoretically and experimentally. They modified the TSI 3025A to operate with DEG and showed
56 particle activation and growth starting from 1 nm in mobility diameter. Because the grown DEG
57 droplets are too small for direct optical detection, a traditional butanol based CPC was used as the
58 droplet detector. The idea of modifying the commercial TSI instrument to operate with DEG has been
59 followed by several other researchers (Jiang et al., 2011a; Jiang et al., 2011b; Kuang et al., 2012a;
60 Kuang et al., 2012b; Wimmer et al., 2013). In 2016 TSI commercialized the DEG based laminar type
61 CPC based on the work of Iida et al. (2009). This instrument, the TSI 3777 nano enhancer (3777), is
62 one of the three instruments characterized in this study.

63 Generally, laminar flow ultrafine CPCs use a sheathed condenser, which makes the CPC design
64 more complex compared to non-sheathed CPCs. Yet recent efforts have shown comparably low
65 detection limits with unsheathed laminar flow instruments. Particle detection with the butanol based
66 TSI 3010 has been shown down to 2.5 nm from the factory settings d50 (diameter at which 50% of
67 sampled particles are detected) of 10 nm (Mertes et al., 1995; Russell et al., 1996; Wiedensohler et
68 al., 1997). Kangasluoma et al. (2015a) showed 1 nm particle detection with the commercial
69 unsheathed laminar type CPCs TSI 3772 and Airmodus A20 by increasing the temperature difference
70 between the saturator and condenser up to 40 °C. The second CPC characterized in this study is a
71 boosted TSI 3010 (B3010), which is a modification of the commercial TSI 3010 developed at the
72 Université Blaise Pascal. In this instrument the temperature control of the saturator and condenser is
73 decoupled to allow free selection of the temperatures, and critical orifice is replaced with a flow meter
74 and a miniature rotary vane pump.

75 The disadvantage of all the previous CPCs is the slight toxicity of the working fluids butanol
76 and DEG, and these organic liquids can introduce contaminant molecules to vapor phase. Hering et al.
77 (2005) addressed this issue by developing a water based, laminar flow technology (Hering and
78 Stolzenburg, 2005), which was commercialized as the TSI WCPC models 3785 (Hering et al., 2005) and
79 3786 (Iida et al., 2008), and subsequently as the models 3783, 3787 and 3788. In the model 3786, and
80 later in the model 3788 (Kupc et al., 2013), 3 nm particle detection was enabled by introducing similar
81 sheathed condenser as in the butanol based CPCs.

82 The ADI versatile WCPC (v-WCPC), which is the third CPC characterized in this study, advances
83 the laminar-flow water-based CPC through a three stage design that reduces the water vapor
84 saturation and temperature in the growth tube after the peak supersaturation is achieved, and yet
85 allows for continued particle growth (Hering et al., 2016). This three-stage approach facilitates higher
86 temperature differences between the first two stages, and can produce higher peak supersaturation
87 values than the ultrafine TSI 3786 or TSI 3788. The v-WCPC is an unsheathed instrument, operating
88 at an aerosol flow rate of 0.3 litres per minute (lpm) and at more extreme temperatures than all of
89 the current commercial TSI WCPCs. In contrast to the DEG-based instruments, which require a
90 separate CPC as a detector due to the small size of the DEG droplets, the droplets formed in the growth
91 tube of the v-WCPC are sufficiently large for direct optical detection.

92 The aim of this study is to make intercomparison experiments for the three new particle
93 counters. Each of the CPCs are operated with different working fluid utilizing different geometries,
94 and first we find the d50 for tungsten oxide test particles for each CPC at temperature settings that
95 they do not detect ions from a radioactive source. As the 3777 and v-WCPC exhibited very similar
96 performance in terms of d50, we conduct further comparison to the two CPCs by testing their
97 response at higher supersaturation than the factory settings, to electrically neutral particles, to
98 organic test particles, and to urban ambient particles. Further, we conducted CPC specific experiments
99 to probe the response of 3777 to varying sample flow relative humidity, of B3010 with various inlet
100 flow rates and of v-WCPC to sampled particle concentration.

101

2 Experimental

2.1 Condensation Particle Counters

A flow diagram of the 3777 is presented in Figure 1. The design is largely similar to the TSI ultrafine 3776. The inlet flow rate is 2.5 lpm, of that 1.5 lpm being transport flow and 1 lpm split as the sheath flow (0.85 lpm) and aerosol flow (0.15 lpm). The sheath flow passes through a dessicant drier to remove most water vapor entering the condenser. Downstream of the drier the sheath flow is saturated with DEG before entering the condenser around the aerosol flow, which is guided in the centre line of the condenser. The saturator has a meandering path in a metal block instead of a porous wick used in ultrafine butanol based CPCs. The 3777 does not have its own optics head, as the droplets formed by DEG condensation are too small for direct detection. Instead the detector is a TSI 3772 CPC, which further enlarges and then counts the droplets pre-grown by DEG in the condenser. The factory settings of the 3777 are: saturator 62 °C and condenser 12 °C (low temperature difference (dT) settings). At these settings the 3777 did not detect any ions produced by a 185 MBq radioactive [241]Am source. It was also operated at boosted settings so that the supersaturation was at the onset of homogeneous nucleation. With the boosted settings the saturator temperature was set to 70 °C and condenser to 7 °C (high dT settings).

Flow diagram of the ADI v-WCPC is presented in Figure 2. The v-WCPC does not require a separate CPC for droplet detection, nor does it use a sheath flow, making it a relatively simple CPC. The v-WCPC has two flows, a transport flow and an aerosol flow, both of which are controlled by critical orifices. For experiments conducted here the inlet flow rate of the v-WCPC was 2.2 lpm, of which 1.9 lpm is transport flow and 0.3 lpm aerosol flow. The aerosol flow passes upward through a three-stage growth tube consisting of a cool-walled conditioner, followed by a short, warm-walled initiator, and subsequently followed by a cool-walled moderator (Hering et al., 2014). A continuous wick spans all three growth tube sections. Liquid water is injected at a rate of 1 µL/min at the initiator, and excess drains toward the inlet and is removed with the transport flow. Peak supersaturation and particle activation occurs within the initiator, and growth continues in the moderator. The formed droplets are counted by an optics head mounted directly at the outlet of the growth tube. Further detail is presented by Hering et al. (2016). The v-WCPC was tested at two different temperature settings: conditioner at 8 °C and initiator at 90 °C (low dT settings), corresponding to supersaturation low enough to not detect any ions from the 185 MBq radioactive [241]Am source, and boosted settings with conditioner at 1 °C and initiator at 95 °C (high dT settings), which is close to the extremes attainable without freezing or boiling. In both instances the moderator was operated at 22°C, and the optics head at 40°C. At the high dT settings both 3777 and v-WCPC are able to detect ions from the [241]Am source.

The B3010 is based on the robust TSI 3010 (Figure 3), from which everything except the saturator block, the condenser and the optical detector are removed. The original electronics have been replaced with custom made boards to handle the higher power consumption, and operate off 28 VDC, the primary power supply in aircrafts. The whole system is controlled by a credit card sized ARM computer, running a tailor-made embedded Linux operating system. It features a touchscreen, a TSI-like serial port protocol, and TTL pulse output. With these modifications the saturator heating and condenser cooling are decoupled. In addition, the critical orifice and external heavy pump are replaced by a laminar flowmeter and a miniature rotary vane pump. The user may set the temperature of the saturator, condenser and optics as well as the flow rate, independently from one another. The B3010 was operated at saturator temperature 55 °C, optics head 56 °C and condenser 11 °C. The B3010 will be described in more detail in a dedicated article, presently in preparation. Table 1 summarizes the instrument operation conditions.

2.2 Direct comparison of all CPCs

153 Two methods were used to generate the test aerosol: glowing wire generator (GWG) and electrospray
154 source. In the GWG (Peineke et al., 2006), a thin, 0.4 mm in diameter, tungsten wire is heated
155 resistively in a metal chamber. The wire is flushed with 5.0 N_2 flow and it has been shown that
156 negatively charged tungsten oxide clusters are formed into the N_2 flow without additional charging
157 (Kangasluoma et al., 2015b). Positively charged clusters contain some hydrocarbon molecules
158 clustered with tungsten oxide, explaining why usually the measured d50 usually is larger for positively
159 than negatively charged clusters (Kangasluoma et al., 2016b). 18 different sizes of particles between
160 1 and 4.5 nm were selected with the Herrmann type high resolution DMA (Kangasluoma et al., 2016a)
161 (Figure 4), and guided to a test CPC and TSI aerosol electrometer (3068B). The tubing lengths
162 downstream of the DMA were selected based on the inlet flow rates so that the particle penetration
163 through the tubes can be assumed equal. The d50 for all three CPCs at low dT settings was measured
164 with tungsten oxide particles.
165
166 2.3 Comparison between the 3777 and the v-WCPC
167
168 The dT of the 3777 and the v-WCPC was increased to the onset of homogeneous droplet formation,
169 and the d50 was measured similarly as described in 2.2 for tungsten oxide particles.
170   To measure the d50 for neutral particles, we followed the approach presented in our previous
171 studies (Kangasluoma et al., 2015b; Kangasluoma et al., 2016b). The sample flow downstream of the
172 DMA passes through a mixing chamber, to which a tube containing a [241]Am radioactive source is
173 connected. 0.2 lpm of the sample flow is drawn through the tube, and ions from the radioactive source
174 are drifted to the mixing chamber against the counter flow with an electric field. A fraction of the
175 sample particles are neutralized by the opposite polarity ions drifted to the mixing chamber. An ion
176 precipitator is placed downstream of the mixing chamber to allow sampling of only neutral particles
177 with the CPC. The concentration detected with the CPC is normalized against the electrometer. The
178 detection efficiency curve is further normalized with detection efficiency at the largest selected
179 diameters where the role of charge on the detection efficiency is assumed to be negligible. This
180 method yields uncertainties in the resulting d50 due to possibly size dependent neutralization
181 efficiency, unknown neutralization mechanism (ion-ion recombination leading to larger physical size,
182 or charge transfer) and chemical composition of the neutralized particles, however, it is currently the
183 only method to measure d50 for neutral particles for sub-3 nm particles. Winkler et al. (2008) used
184 similar method to measure nucleation probabilities of electrically charged and neutral clusters, the
185 difference being that they used bipolar neutralizer. Neutral d50 was measured for both instruments
186 with high and low dT by neutralizing both negatively and positively charged particles.
187   To test the response of the 3777 and the v-WCPC to organic test particles,
188 tetradodecylammonium bromide (TDDABr) (Ude and Fernández de la Mora, 2005) particles were
189 generated with an electrospray source. The electrospray source produces droplets, which contain the
190 sample molecules, by spraying liquid at high voltage out of a capillary needle against a grounded
191 electrode. The charged droplets are close to the Rayleigh limit, and produce charged sample molecules
192 and clusters to the gas flow by series of Coulomb explosions, and ion and solvent evaporation from
193 the droplet. The highly charged droplets can be close to 2 nm in mobility diameter (Ude and Fernández
194 de la Mora, 2005), for which we neutralized the flow exiting the electrospray with a radioactive [241]Am
195 source to also be able to sample the singly charged clusters which are larger than 2 nm (Kangasluoma
196 et al., 2016a). d50 was measured for the 3777 and v-WCPC for positively charged TDDABr with the low
197 dT settings, and for the v-WCPC at the high dT settings. For the 3777 we could not measure the d50
198 at high dT settings due to the fact that the aerosol-to-sheath flow ratio is very sensitive to the CPC
199 inlet pressure, and TDDABr was produced by drawing the flow out of the DMA, leading to a pressure
200 drop of approximately 5 kPa at the CPC inlets. This pressure drop was enough to alter the aerosol-to-
201 sheath flow ratio in the 3777 and cause homogeneous droplet formation at high dT settings.
202   Finally, the 3777 and v-WCPC were placed to sample atmospheric aerosol from Helsinki city
203 area. The instruments were sampling from the same inlet for approximately 18 h to compare the

204 measured concentrations from atmospheric aerosol. The v-WCPC data were dead-time corrected
205 using the dead time correction factor derived from the concentration dependent response for 4.4 nm
206 (see next chapter).
207
208 2.4 CPC specific tests
209
210 As previous literature has reported that water vapor in the sample flow can affect the detection
211 efficiency a DEG based CPC (Iida et al., 2009; Kangasluoma et al., 2013), we measured the d50 of the
212 3777 at various sample flow dew points. Water vapor was added to the sample flow with a humidified
213 dilution flow downstream of the DMA. The d50 of the 3777 was measured at four different sample
214 flow dew points with negatively charged tungsten oxide particles.
215   Based on previous literature (Kangasluoma et al., 2015a), the detection efficiency of the
216 laminar type butanol CPCs can be increased by increasing the inlet flow rate. We tested the
217 performance of the B3010 at four different inlet flow rates. The d50 for the B3010 was measured at
218 inlet flow rates, 0.5, 1.0, 1.4 and 1.6 lpm, by varying the rotary vane pump speed.
219   Water based CPCs are known to be sensitive for vapor depletion effects (Lewis and Hering,
220 2013). Therefore the response of the v-WCPC was measured against the TSI electrometer (model
221 3068B) for different concentrations at sizes 1.4nm, 1.8nm, 2.4nm and 4.4 nm. The concentration at
222 each size was controlled by adding a dilution flow of compressed and filtered air downstream of the
223 DMA. Simultaneous data were collected for the 3777, however the dilution flow was again enough to
224 change the aerosol-to-sheath flow ratio of the 3777 due to a small change in the inlet pressure, and
225 therefore the 3777 data of this experiment are not presented. However, assuming that any possible
226 undercounting at high concentration originates from particle coincidence in the optics, the
227 concentration calibration of the 3777 should be practically the same as of the 3772 CPC when the
228 dilution of 0.15/1 is taken into account.
229
230 3 Results
231
232 3.1 Direct comparison of all CPCs
233
234 Figure 5 presents the d50 curves for the B3010, 3777 and v-WCPC at low dT settings for positively and
235 negatively charged tungsten oxide particles. The standard deviation in the detection efficiency data
236 was in most cases < 5%, which is why we do not plot detection efficiency error bars. X-axis uncertainty
237 can be taken from the Herrmann DMA resolution of approximately 20, leading to relative uncertainty
238 of ± 2%, which is the square root of variance of the normal distribution fitted to the
239 tetraheptylammonium bromide positively charged monomer peak. Therefore, uncertainties in the
240 data arise mostly from other sources, such as possibly unequal sampling line penetration or possibly
241 changing particle chemical composition as a function of size. At these settings none of the CPCs detect
242 the ions generated by a bipolar ion source. We find that the v-WCPC exhibits slightly lower d50 than
243 the 3777, while the d50 of the B3010 is clearly the highest. The d50 of 3.2 – 3.4 nm for the B3010,
244 however, shows that the conventional TSI 3010 can be boosted to similar performance as the TSI
245 ultrafine 3776, just with a shallower d50 curve due to larger particle diffusion losses, by decoupling
246 the heating and cooling of the saturator and condenser. Respective d50 values for the B3010, v-WCPC
247 and TSI-3777 are 3.4 nm, 1.7 nm and 1.8 nm for negatively charged tungsten oxide, and 3.2 nm, 1.9
248 nm and 2.0 nm for positively charged.
249
250 3.2 Comparison between the 3777 and the v-WCPC
251
252 At high dT settings the d50 curves are presented in Figure 6. For the 3777 the temperatures were
253 selected as those that are just below the limit of homogeneous nucleation of the DEG working fluid.
254 For the v-WCPC, the temperatures are simply the largest extremes attainable without freezing or

255 boiling the water working fluid. Unlike the DEG instrument, the high dT operation of the v-WCPC is
256 not near the homogeneous nucleation limit, as no evidence of homogeneous nucleation was observed
257 even at reduced inlet pressures. At these higher dT settings, we find somewhat more efficient
258 detection of smaller particles by the 3777 than the v-WCPC. The d50s are lowered to 1.4 nm and 1.3
259 nm for negatively charged, and to 1.5 nm and 1.4 nm for positively charged for the v-WCPC and 3777,
260 respectively.

261   Table 2 summarizes the measured d50 for all experiments. The d50 for 3777 and v-WCPC at
262 both settings is lower for negatively charged particles than for positively charged particles. This is
263 observed throughout the past literature (Stolzenburg and McMurry, 1991; Winkler et al., 2008; Sipilä
264 et al., 2009; Kuang et al., 2012b; Kangasluoma et al., 2014), and explained by hydrocarbon
265 contaminants in the positively charged particles (Kangasluoma et al., 2016b). Based on previous
266 literature (Kuang et al., 2012b; Kangasluoma et al., 2014) slightly lower d50 values can be expected
267 for inorganic salt particles than the measured d50s for tungsten oxide particles in this study. TSI states
268 in their instrument brochure a d50 of 1.4 nm for negatively charged NaCl particles at factory settings
269 (low dT in this study), which is well in line with this study. Similarly, the d50 values reported here for
270 the v-WCPC are close to those observed by Hering et al. (2016) who measured d50 of 1.6 nm and
271 1.9 nm for high dT and low dT operation, respectively, for particles from a heated NiCr wire.

272   Figure 7 presents the d50 curves measured with the neutralized tungsten oxide particles for
273 3777 and v-WCPC. The data is normalized so that the mean detection efficiency at 3 largest diameters
274 is 90% based on the assumption that at those sizes the particle charge does not affect the detection
275 efficiency anymore. Also is assumed, through the normalization that the neutralization efficiency does
276 not change as a function of the particle size. Further uncertainties arise from the unknown processes
277 that take place during neutralization. Due to these uncertainties, the curves are not as smooth as for
278 the charged particles. However, an estimate for the neutral d50 will be obtained from these
279 experiments, which are 1.6 nm and 1.5 nm for v-WCPC and 3777 at high dT, and 2.0 nm and 1.9 nm at
280 low dT settings, respectively, for neutralized negatively charged tungsten oxide. For neutralized
281 positively charged particles the respective values are 2.2 nm and 2.1 nm at high dT settings and 2.4
282 nm and 2.3 nm at low dT settings (Figure 8). The difference in the d50s between the negatively and
283 positively charged particles after neutralization are possibly mostly explained by their differences in
284 the chemical composition. Positively charged particles contain more contaminant species than the
285 negatively charged particles, which is still observed in the d50 when they both are neutralized. For
286 more details, refer to Kangasluoma et al. (2016b). The neutral d50s are greater than for charged d50
287 values by approximately 0.1-0.5 nm at low dT settings, similar to the values obtained in Kangasluoma
288 et al. (2016b) for water-tungsten oxide and DEG-tungsten oxide system.

289   The d50 curves for positively charged TDDABr for the 3777 and v-WCPC are presented in
290 Figure 9. For both instruments the d50 values are higher than for tungsten oxide particles, but this is
291 most pronounced for the v-WCPC. At the low dT settings d50 values are 3.3 nm and 2.5 nm at for the
292 v-WCPC and 3777 respectively, and 2.8 nm for the v-WCPC at high dT. At the high dT and the reduced
293 inlet pressure for these TDDABr tests, the 3777 produced homogeneously nucleated particles, and
294 hence its high dT d50 value could not be measured. To obtain accurate particle concentration
295 measurements, these differences in the d50 imply that the CPCs should be calibrated with the same
296 aerosol composition as the real experiment is conducted.

297   A fraction of the data measured from atmospheric aerosol is presented in Figure 10. The
298 measurement location is above a bus stop, which several busses pass daily through. The bus stop times
299 are marked to the figure. The background aerosol concentration during that morning was around
300 3 000 – 10 000 cm^{-3}. Clear spikes up to 200 000 cm^{-3} in the measured concentrations are observed
301 throughout the morning. The number concentration is generally high during traffic hours, and both
302 CPCs reacts instantaneously to the occasional spikes in the number concentration. From the data of
303 Figure 10, a correlation plot between the v-WCPC and 3777 is presented in Figure 11 for
304 concentrations below 50 000 cm^{-3}. With R^2 of 0.99 the two CPCs show remarkably good agreement
305 with slope of 1.02 and offset of 340 up to concentrations of 50 000 cm^{-3}.

306
307   3.2 CPC specific tests

308

309   Because water vapor has been observed to alter the d50 in the original laminar flow DEG instruments,
310   this question was examined for the 3777. The response of the 3777 for negatively charged tungsten
311   oxide particles as a function of sample flow dew point is presented in Figure 12. The observed variation
312   with dew points ranging from completely dry gas to 20 °C in the d50 is only approximately 0.1 nm. The
313   apparently increased plateau value for the highest dew point can be due to slightly higher inlet
314   pressure, increasing the aerosol flow of the instrument. The variation in the d50 due to changing dew
315   point is less than compared to for example 0.3 nm reported in Kangasluoma et al. (2013) for the
316   Airmodus A09 PSM. This is due to the smaller amount of sample flow water vapor reaching the
317   condenser in the 3777, since 85% of the condenser flow is dried, as compared to 0% of the condenser
318   flow of the PSM of that time.
319   Results from the inlet flow rate experiment for the B3010 is presented in Figure 13. The d50
320   curve at aerosol flow rates of, 1, 1.4 and 1.6 lpm are rather similar within the experimental
321   uncertainties, while at flow rate of 0.5 the detection efficiency clearly deviates to lower values at
322   particle diameters larger than 3 nm. This can be possibly due to larger final droplet diameters and
323   subsequent gravitational losses at the low flow rate. Similar increase in the detection efficiency with
324   higher flow rate as in Kangasluoma et al. (2015a) was not observed, which can be due to the
325   differences in the saturator designs between the 3010 and 3772: 3010 has a single hole reservoir type
326   saturator while 3772 has 8 hole multitube saturator which possibly saturates the sample flow better
327   than the one hole saturator at higher flow rates.
328   As with all CPCs, the peak supersaturation, and hence the lowest detectable particle size can
329   be affected by the presence of other particles in the flow due to a combination of condensational heat
330   release and vapor depletion. These effects for the original WCPCs were explored by Lewis and Hering
331   (2013), and is evaluated here for the v-WCPC. Figure 14 shows the concentration dependent response
332   at four particle sizes for the v-WCPC. The maximum concentration at each size was determined by the
333   maximum concentration we were able to pass through the DMA. The data are corrected for dead
334   time, as described by Hering et al. (2005), and as is standard for most of the commercial CPCs. This
335   approach uses the instrument dead time multiplied by a dead time correction factor, which accounts
336   for the increase in effective dead time due to overlapping tails in pulses below the threshold. For this
337   data set the dead time correction factor was set to 1.23 to yield a linear response to concentration at
338   4.4 nm. Then this same dead time correction factor was applied to measurements at other sizes. The
339   curves of the three smallest particle sizes have a negative slope due to the reduction in
340   supersaturation at high concentrations caused by condensational heating (Lewis and Hering, 2013).
341   However, the effect is relatively small, with the detection efficiency at 1.8 nm dropping from 36% at a
342   concentration of 3000cm^{-3} to 33% at a concentration of 90000cm^{-3}.

343

344   4 Conclusions

345

346   Three new sub-3 nm CPCs, boosted 3010 type CPC, ADI versatile water CPC and the TSI 3777 nano
347   enhancer were characterized for the d50 diameter. The boosted 3010 type CPC was shown to be able
348   to detect tungsten oxide particles smaller than 3 nm. The v-WCPC and 3777 were characterized with
349   similar test aerosols with two different settings: low dT settings set so that the CPCs did not detect
350   any ions from a radioactive charger, and high dT settings set either so that the supersaturation was at
351   the onset of homogeneous droplet formation (3777) or set to the largest value that avoids freezing or
352   boiling (v-WCPC). The d50 diameters for tungsten oxide were found to range from 1.7 nm to 2.4 nm
353   at low dT and from 1.4 nm to 2.2 nm at high dT for the v-WCPC. For the 3777 the d50 ranged from 1.8
354   nm to 2.3 nm at low dT and from 1.3 nm to 2.1 nm at high dT. Both CPCs were observed to detect
355   charged tungsten oxide particles better than neutral ones. The organic salt particles (TDDABr) were
356   detected less efficiently, with low dT d50 diameters of 3.3 nm for the v-WCPC, and 2.5 nm for the TSI-

357 3777. When measuring the same atmospheric aerosol the two CPCs showed a very good agreement
358 with regression slope of 1.02 and R^2 of 0.99.
359   From the results we can make the following conclusions: The TSI 3010 hardware can be tuned
360 to accomplish 3 nm particle detection by increasing the dT but not by increasing the inlet flow rate,
361 which is in line with Buzorius (2001). This is possibly due to imperfect flow saturation in the reservoir
362 type saturator as opposed to the multihole saturator of TSI 3772 and planar type saturator of
363 Airmodus A20 (Kangasluoma et al., 2015a). Due to the variations in the d50 with test particle
364 composition for the v-WCPC and 3777, a careful CPC calibration should be conducted with the same
365 particle composition as of the sampled particles. If the composition of the sampled particles is
366 completely unknown, the obtained particle concentrations at the size range of the d50 can have
367 significant uncertainties. The effect of particle charge on the d50 was shown to be up to approximately
368 0.5 nm, which has implications on to system characterizations where the fraction of charged particles
369 can be expected to be high (Wang et al., 2017), or CPC calibration is conducted with charged particles
370 and sampled particles are neutral, and high precision d50 is required.
371

372 Acknowledgements
373
374 The authors acknowledge TSI Inc. who provided the control boards and optics for the v-WCPC, and
375 who loaned the TSI 3777 for these experiments. The research was partly funded by European Research
376 Council (ATMNUCLE, 227463), Academy of Finland (Center of Excellence Program projects 1118615
377 and 139656), European Commission seventh Framework program (ACTRIS2 contract no 654109, PPP
378 and EUROCHAMP-2020), Labex ClerVolc contribution n° 228 and Maj and Tor Nessling Foundation
379 (grant 201700296).
380

381 References
382
383 Aalto, P., Hameri, K., Becker, E., Weber, R., Salm, J., Makela, J. M., Hoell, C., O'Dowd, C. D., Karlsson,
384 H., Hansson, H. C., Vakeva, M., Koponen, I. K., Buzorius, G., and Kulmala, M.: Physical
385 characterization of aerosol particles during nucleation events, Tellus B, 53, 344-358, 2001.

386
387 Buzorius, G.: Cut-off sizes and time constants of the CPC TSI 3010 operating at 1-3 lpm flow rates,
388 Aerosol Sci Tech, 35, 577-585, 2001.

389
390 Hering, S. V. and Stolzenburg, M. R.: A method for particle size amplification by water condensation
391 in a laminar, thermally diffusive flow, Aerosol Sci Tech, 39, 428-436, 2005.

392
393 Hering, S. V., Stolzenburg, M. R., Quant, F. R., Oberreit, D. R., and Keady, P. B.: A laminar-flow, water-
394 based condensation particle counter (WCPC), Aerosol Sci Tech, 39, 659-672, 2005.

395
396 Hering, S. V., Spielman, S. R., and Lewis, G. S.: Moderated, Water-Based, Condensational Particle
397 Growth in a Laminar Flow, Aerosol Sci Tech, 48, 401-408, 2014.

398
399 Hering, S. V., Lewis, G. L., Spielman, S. R., Eiguren-Fernandez, A., Kreisberg, N. M., Kuang, C., and
400 Attoui, M.: Detection near 1-nm with a Laminar-Flow, Water-Based Condensation Particle Counter,
401 Aerosol Sci Tech, 2016. 2016.

402
403 Iida, K., Stolzenburg, M. R., McMurry, P. H., Smith, J. N., Quant, F. R., Oberreit, D. R., Keady, P. B.,
404 Eiguren-Fernandez, A., Lewis, G. S., Kreisberg, N. M., and Hering, S. V.: An ultrafine, water-based

405 condensation particle counter and its evaluation under field conditions, Aerosol Sci Tech, 42, 862-
406 871, 2008.

407

408 Iida, K., Stolzenburg, M. R., and McMurry, P. H.: Effect of Working Fluid on Sub-2 nm Particle
409 Detection with a Laminar Flow Ultrafine Condensation Particle Counter, Aerosol Sci Tech, 43, 81-96,
410 2009.

411

412 Jiang, J. K., Chen, M. D., Kuang, C. A., Attoui, M., and McMurry, P. H.: Electrical Mobility
413 Spectrometer Using a Diethylene Glycol Condensation Particle Counter for Measurement of Aerosol
414 Size Distributions Down to 1 nm, Aerosol Sci Tech, 45, 510-521, 2011a.

415

416 Jiang, J. K., Zhao, J., Chen, M. D., Eisele, F. L., Scheckman, J., Williams, B. J., Kuang, C. A., and
417 McMurry, P. H.: First Measurements of Neutral Atmospheric Cluster and 1-2 nm Particle Number
418 Size Distributions During Nucleation Events, Aerosol Sci Tech, 45, Ii-V, 2011b.

419

420 Kangasluoma, J., Junninen, H., Lehtipalo, K., Mikkilä, J., Vanhanen, J., Attoui, M., Sipilä, M., Worsnop,
421 D., Kulmala, M., and Petäjä, T.: Remarks on Ion Generation for CPC Detection Efficiency Studies in
422 Sub-3-nm Size Range, Aerosol Sci Tech, 47, 556-563, 2013.

423

424 Kangasluoma, J., Kuang, C., Wimmer, D., Rissanen, M. P., Lehtipalo, K., Ehn, M., Worsnop, D. R.,
425 Wang, J., Kulmala, M., and Petäjä, T.: Sub-3 nm particle size and composition dependent response of
426 a nano-CPC battery, Atmos Meas Tech, 7, 689-700, 2014.

427

428 Kangasluoma, J., Ahonen, L., Attoui, M., Vuollekoski, H., Kulmala, M., and Petäjä, T.: Sub-3 nm
429 Particle Detection with Commercial TSI 3772 and Airmodus A20 Fine Condensation Particle Counters,
430 Aerosol Sci Tech, 49, 674-681, 2015a.

431

432 Kangasluoma, J., Attoui, M., Junninen, H., Lehtipalo, K., Samodurov, A., Korhonen, F., Sarnela, N.,
433 Schmidt-Ott, A., Worsnop, D., Kulmala, M., and Petäjä, T.: Sizing of neutral sub 3 nm tungsten oxide
434 clusters using Airmodus Particle Size Magnifier, J Aerosol Sci, 87, 53-62, 2015b.

435

436 Kangasluoma, J., Attoui, M., Korhonen, F., Ahonen, L., Siivola, E., and Petäjä, T.: Characterization of a
437 Herrmann type high resolution differential mobility analyzer, Aerosol Sci Tech, 50, 222-229, 2016a.

438

439 Kangasluoma, J., Samodurov, A., Attoui, M., Franchin, A., Junninen, H., Korhonen, F., Kurtén, T.,
440 Vehkamäki, H., Sipilä, M., Lehtipalo, K., Worsnop, D., Petäjä, T., and Kulmala, M.: Heterogeneous
441 nucleation onto ions and neutralized ions - insights into sign-preference, Journal of Physical
442 Chemistry C, 120, 7444-7450, 2016b.

443

444 Kuang, C., Chen, M., Zhao, J., Smith, J., McMurry, P. H., and Wang, J.: Size and time-resolved growth
445 rate measurements of 1 to 5 nm freshly formed atmospheric nuclei, Atmos Chem Phys, 12, 3573-
446 3589, 2012a.

447

448 Kuang, C., Chen, M. D., McMurry, P. H., and Wang, J.: Modification of Laminar Flow Ultrafine
449 Condensation Particle Counters for the Enhanced Detection of 1 nm Condensation Nuclei, Aerosol
450 Sci Tech, 46, 309-315, 2012b.

451
452 Kupc, A., Bischof, O., Tritscher, T., Beeston, M., Krinke, T., and Wagner, P. E.: Laboratory
453 Characterization of a New Nano-Water-Based CPC 3788 and Performance Comparison to an
454 Ultrafine Butanol-Based CPC 3776, Aerosol Sci Tech, 47, 183-191, 2013.

455
456 Lewis, G. S. and Hering, S. V.: Minimizing Concentration Effects in Water-Based, Laminar-Flow
457 Condensation Particle Counters, Aerosol Sci Tech, 47, 645-654, 2013.

458
459 Mertes, S., Schroder, F., and Wiedensohler, A.: The Particle-Detection Efficiency Curve of the Tsi-
460 3010 Cpc as a Function of the Temperature Difference between Saturator and Condenser, Aerosol
461 Sci Tech, 23, 257-261, 1995.

462
463 Okuyama, K., Kousaka, Y., and Motouchi, T.: Condensational Growth of Ultrafine Aerosol-Particles in
464 a New Particle-Size Magnifier, Aerosol Sci Tech, 3, 353-366, 1984.

465
466 Peineke, C., Attoui, M. B., and Schmidt-Ott, A.: Using a glowing wire generator for production of
467 charged, uniformly sized nanoparticles at high concentrations, J Aerosol Sci, 37, 1651-1661, 2006.

468
469 Russell, L. M., Zhang, S. H., Flagan, R. C., Seinfeld, J. H., Stolzenburg, M. R., and Caldow, R.: Radially
470 classified aerosol detector for aircraft-based submicron aerosol measurements, J Atmos Ocean Tech,
471 13, 598-609, 1996.

472
473 Seto, T., Okuyama, K., de Juan, L., and Fernández de la Mora, J.: Condensation of supersaturated
474 vapors on monovalent and divalent ions on varying size, J Chem Phys, 107, 1576-1585, 1997.

475
476 Sipilä, M., Lehtipalo, K., Attoui, M., Neitola, K., Petäjä, T., Aalto, P. P., O'Dowd, C. D., and Kulmala, M.:
477 Laboratory Verification of PH-CPC's Ability to Monitor Atmospheric Sub-3 nm Clusters, Aerosol Sci
478 Tech, 43, 126-135, 2009.

479
480 Stolzenburg, M. R. and McMurry, P. H.: An Ultrafine Aerosol Condensation Nucleus Counter, Aerosol
481 Sci Tech, 14, 48-65, 1991.

482
483 Ude, S. and Fernández de la Mora, J.: Molecular monodisperse mobility and mass standards from
484 electrosprays of tetra-alkyl ammonium halides, J Aerosol Sci, 36, 1224-1237, 2005.

485
486 Vanhanen, J., Mikkilä, J., Lehtipalo, K., Sipilä, M., Manninen, H. E., Siivola, E., Petäjä, T., and Kulmala,
487 M.: Particle Size Magnifier for Nano-CN Detection, Aerosol Sci Tech, 45, 533-542, 2011.

488
489 Wang, Y., Kangasluoma, J., Attoui, M., Fang, J., Junninen, H., Kulmala, M., Petäjä, T., and Biswas, P.:
490 The high charge fraction of flame-generated particles in the size range below 3 nm measured by
491 enhanced particle detectors, Combust Flame, 176, 72-80, 2017.

492

493 Weber, R. J., Marti, J. J., McMurry, P. H., Eisele, F. L., Tanner, D. J., and Jefferson, A.: Measured
494 atmospheric new particle formation rates: Implications for nucleation mechanisms, Chem Eng
495 Commun, 151, 53-64, 1996.

496

497 Wiedensohler, A., Orsini, D., Covert, D. S., Coffmann, D., Cantrell, W., Havlicek, M., Brechtel, F. J.,
498 Russell, L. M., Weber, R. J., Gras, J., Hudson, J. G., and Litchy, M.: Intercomparison study of the size-
499 dependent counting efficiency of 26 condensation particle counters, Aerosol Sci Tech, 27, 224-242,
500 1997.

501

502 Wilson, J. C., Blackshear, E. D., and Hyun, J. H.: An Improved Continuous-Flow Condensation Nucleus
503 Counter for Use in the Stratosphere, J Aerosol Sci, 14, 387-391, 1983.

504

505 Wimmer, D., Lehtipalo, K., Franchin, A., Kangasluoma, J., Kreissl, F., Kurten, A., Kupc, A., Metzger, A.,
506 Mikkilä, J., Petäjä, T., Riccobono, F., Vanhanen, J., Kulmala, M., and Curtius, J.: Performance of
507 diethylene glycol-based particle counters in the sub-3 nm size range, Atmos Meas Tech, 6, 1793-
508 1804, 2013.

509

510 Winkler, P. M., Steiner, G., Vrtala, A., Vehkamäki, H., Noppel, M., Lehtinen, K. E. J., Reischl, G. P.,
511 Wagner, P. E., and Kulmala, M.: Heterogeneous nucleation experiments bridging the scale from
512 molecular ion clusters to nanoparticles, Science, 319, 1374-1377, 2008.

513

514
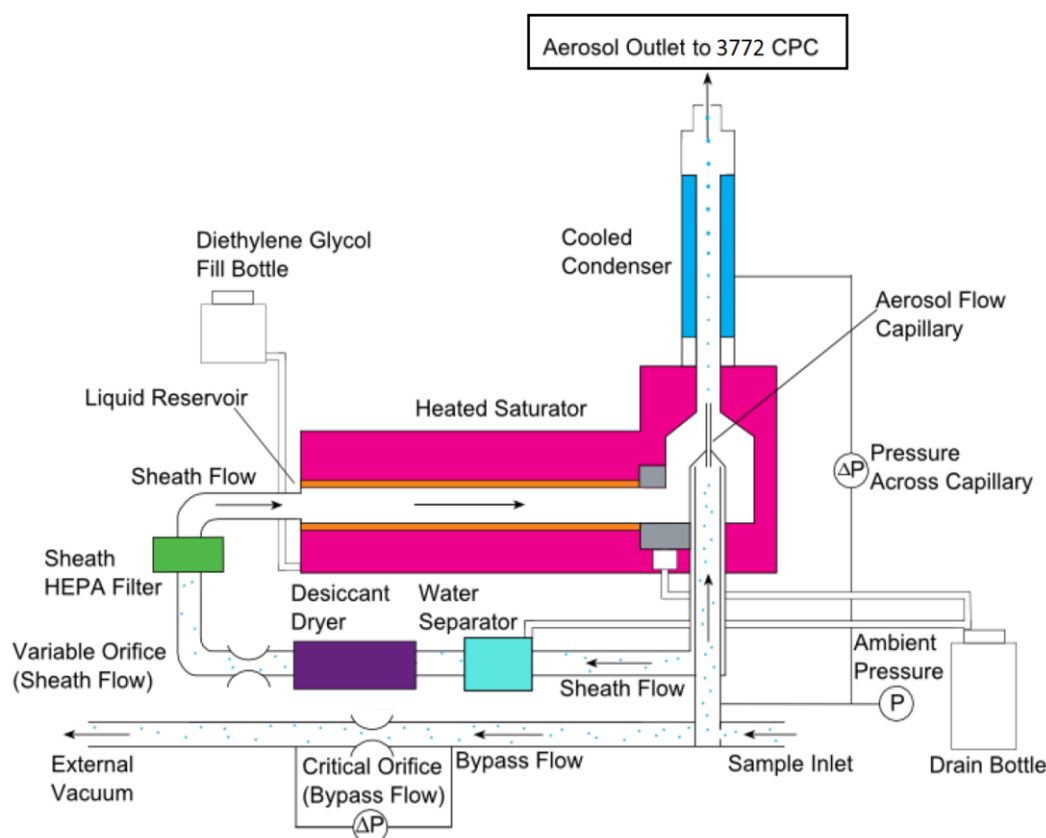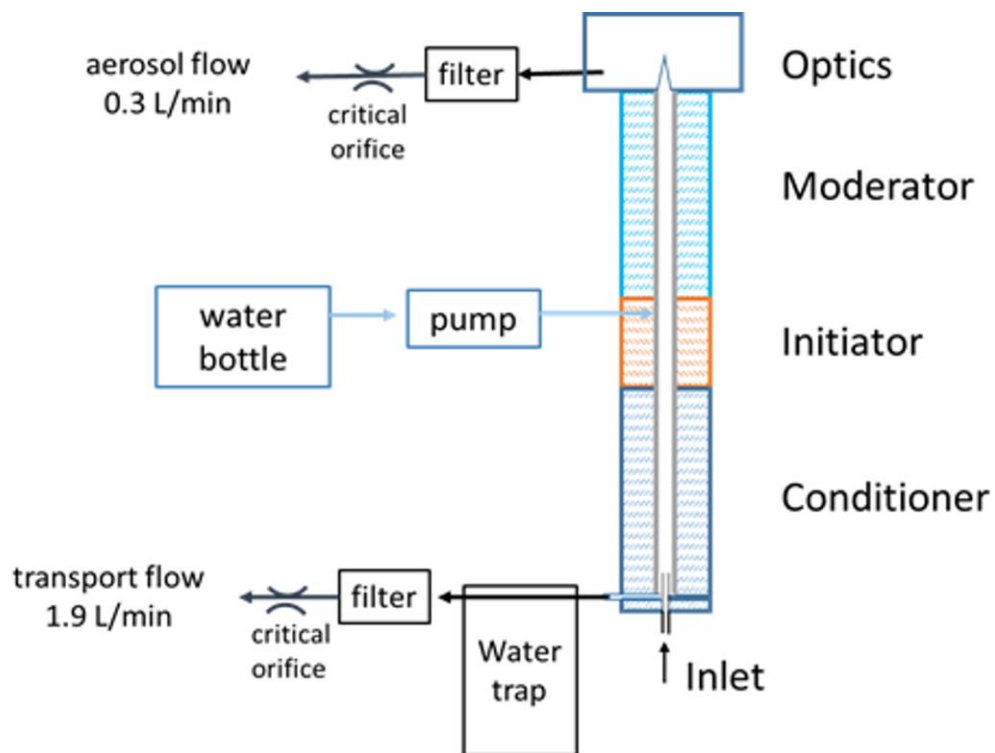
515
516 Figure 1. TSI 3777 nano enhancer (courtesy of TSI Inc.)

517

518
519   Figure 2. ADI v-WCPC
520

521
522   Figure 3. B3010.
523
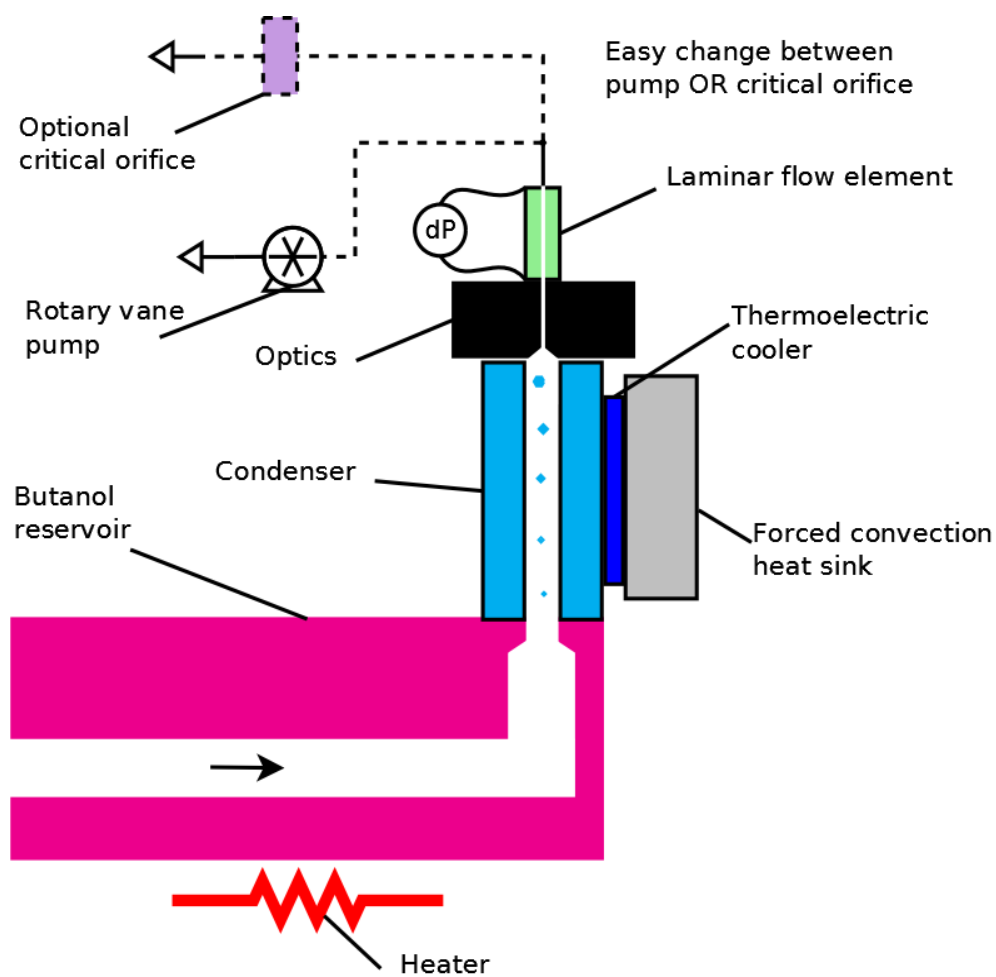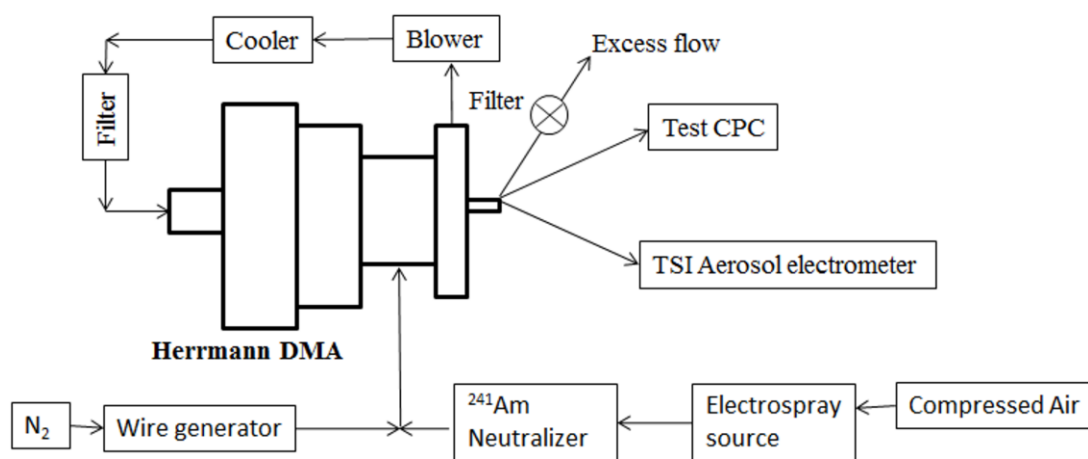
524
525   Figure 4. Experimental setup to measure d50 for charged particles
526
527
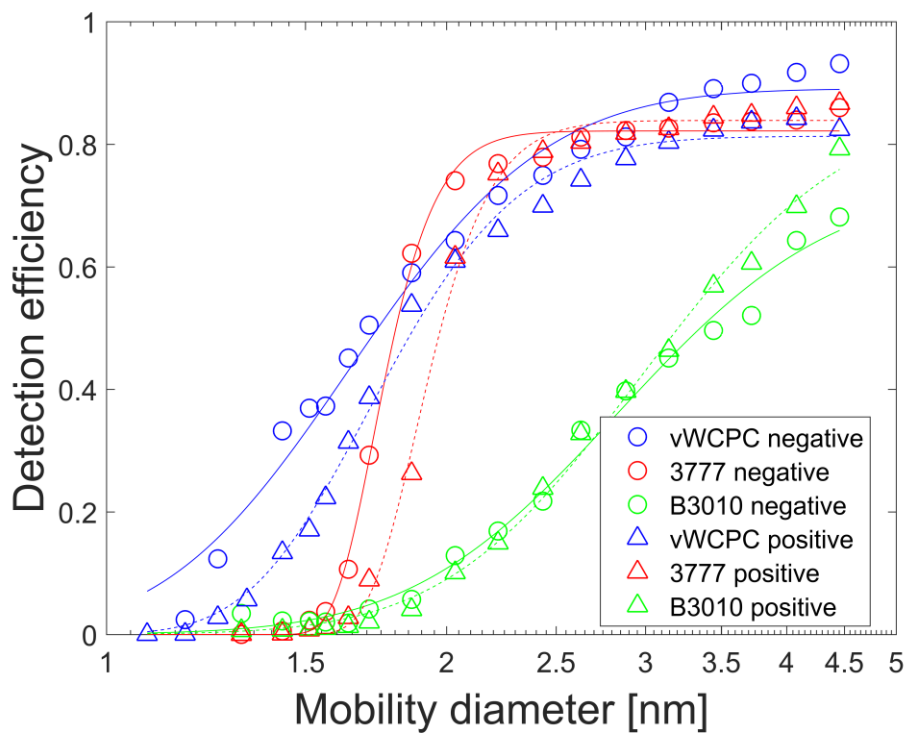
528
529 Figure 5. Detection efficiency of the CPCs as a function of size for negatively and positively charged
530 tungsten oxide particles at low dT settings.
531
532
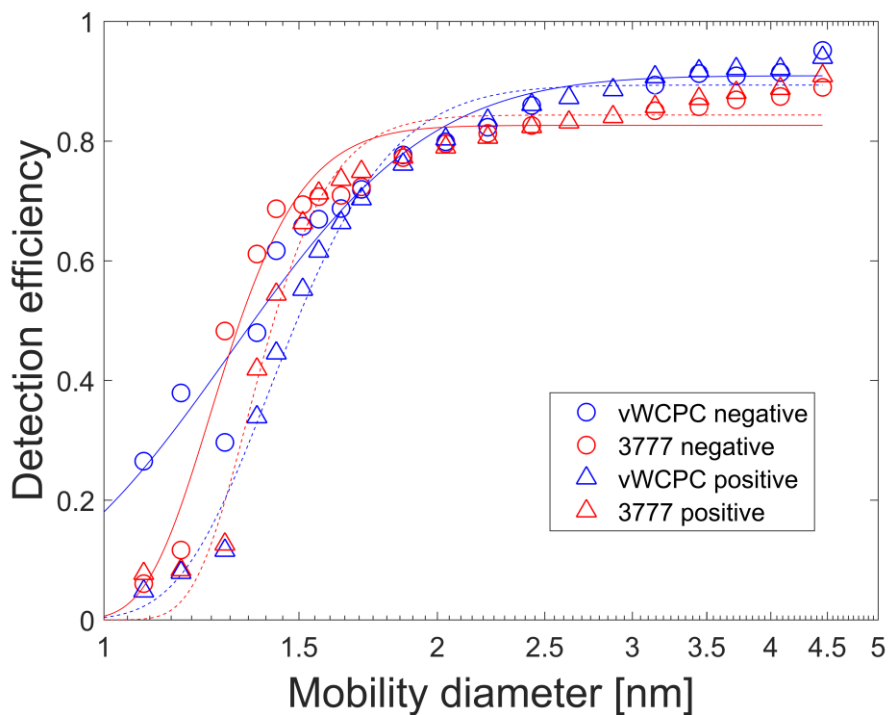
533
534 Figure 6. Detection efficiency of the CPCs as a function of size for positively and negatively charged
535 tungsten oxide particles at high dT settings.
536
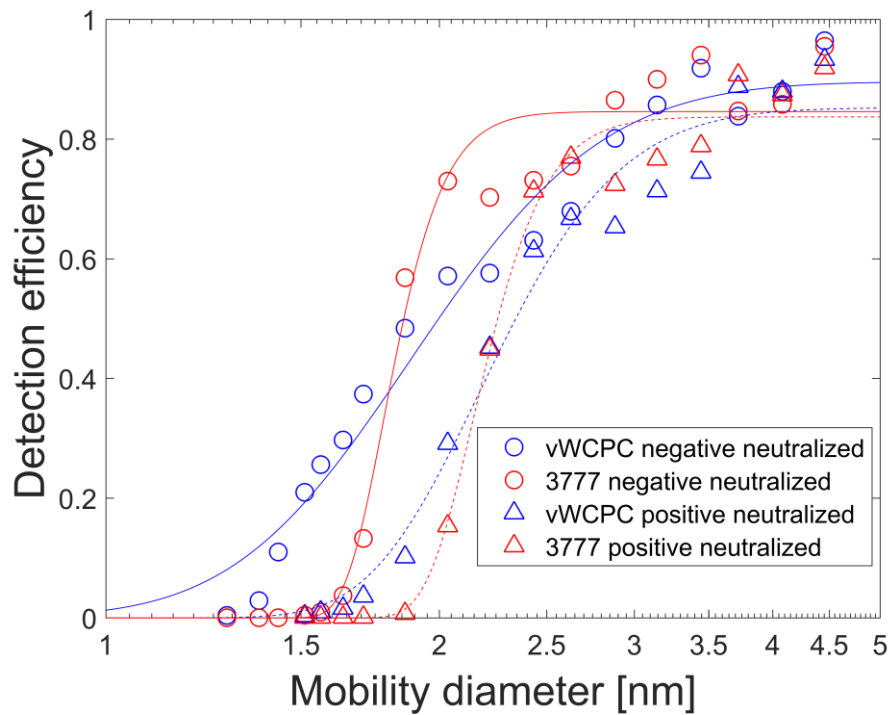
537
538 Figure 7. Detection efficiency of the CPCs as a function of size for negatively and positively charged
539 tungsten oxide particles that are neutralized at low dT settings.
540
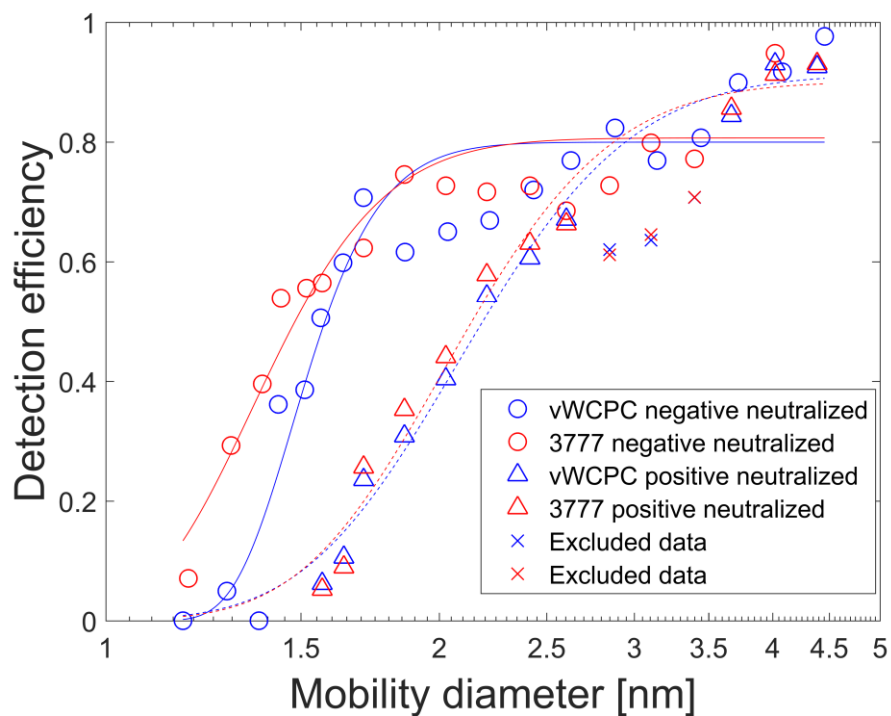
541
542 Figure 8. Detection efficiency of the CPCs as a function of size for negatively and positively charged
543 tungsten oxide particles that are neutralized at high dT settings.
544
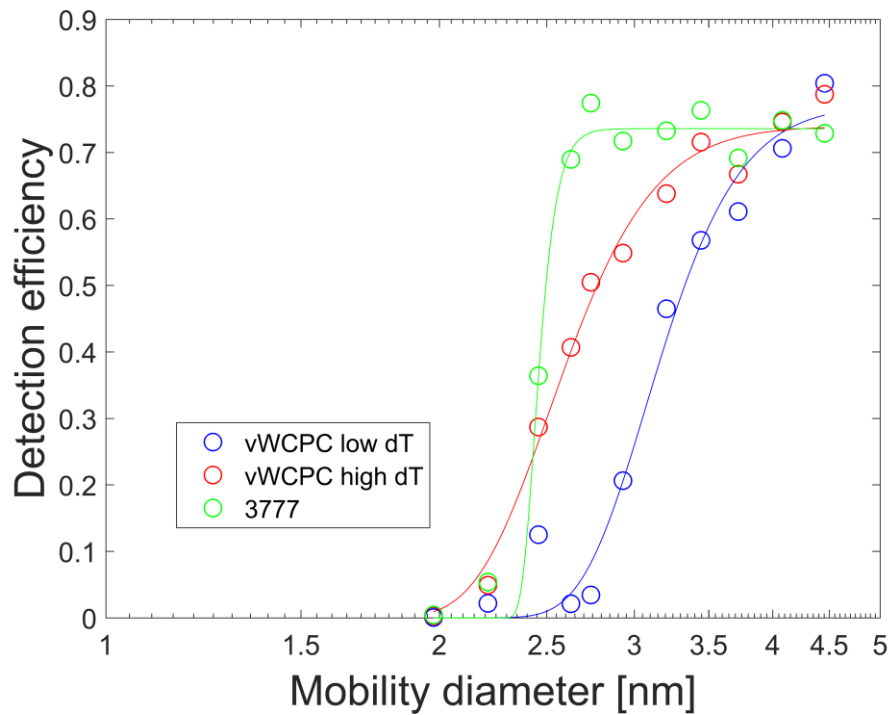
545
546   Figure 9. Detection efficiency of the CPCs as a function of size for positively charged TDDABr particles
547   at low and high dT settings for v-WCPC and at low dT settings for the 3777.
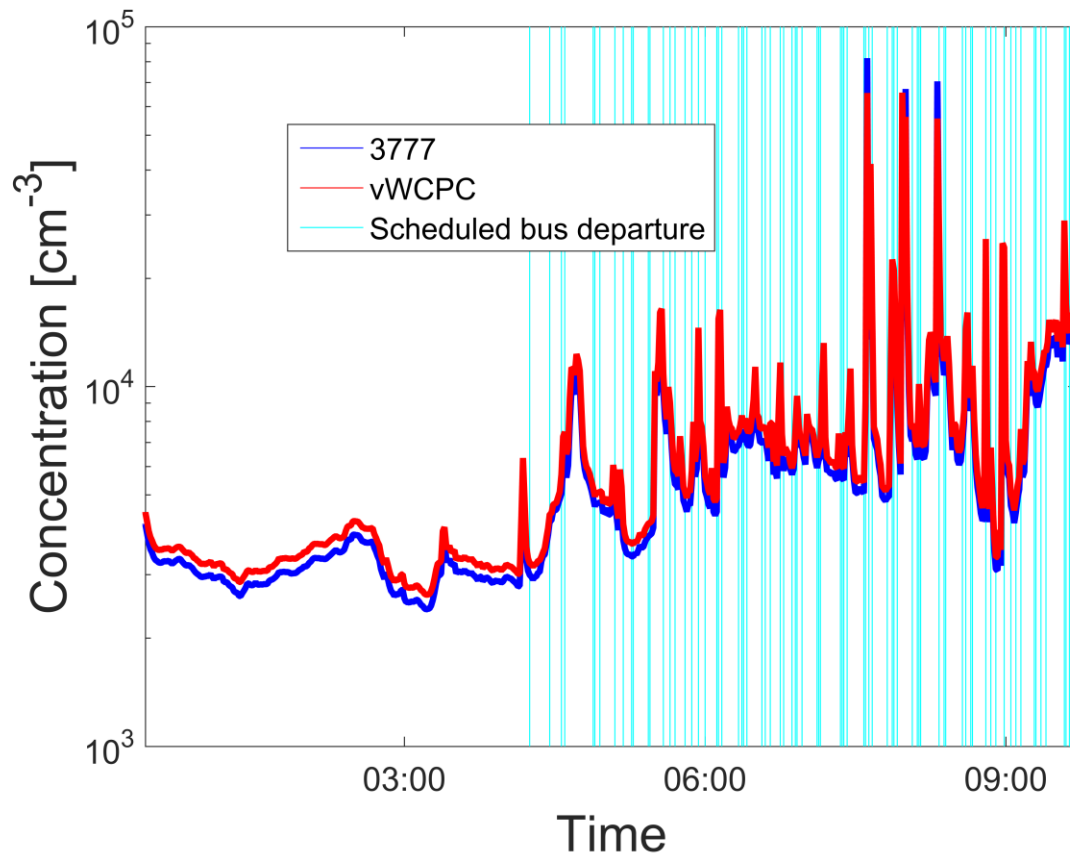
548
549   Figure 10. Concentration measured by the 3777 and v-WCPC from urban atmospheric air.
550
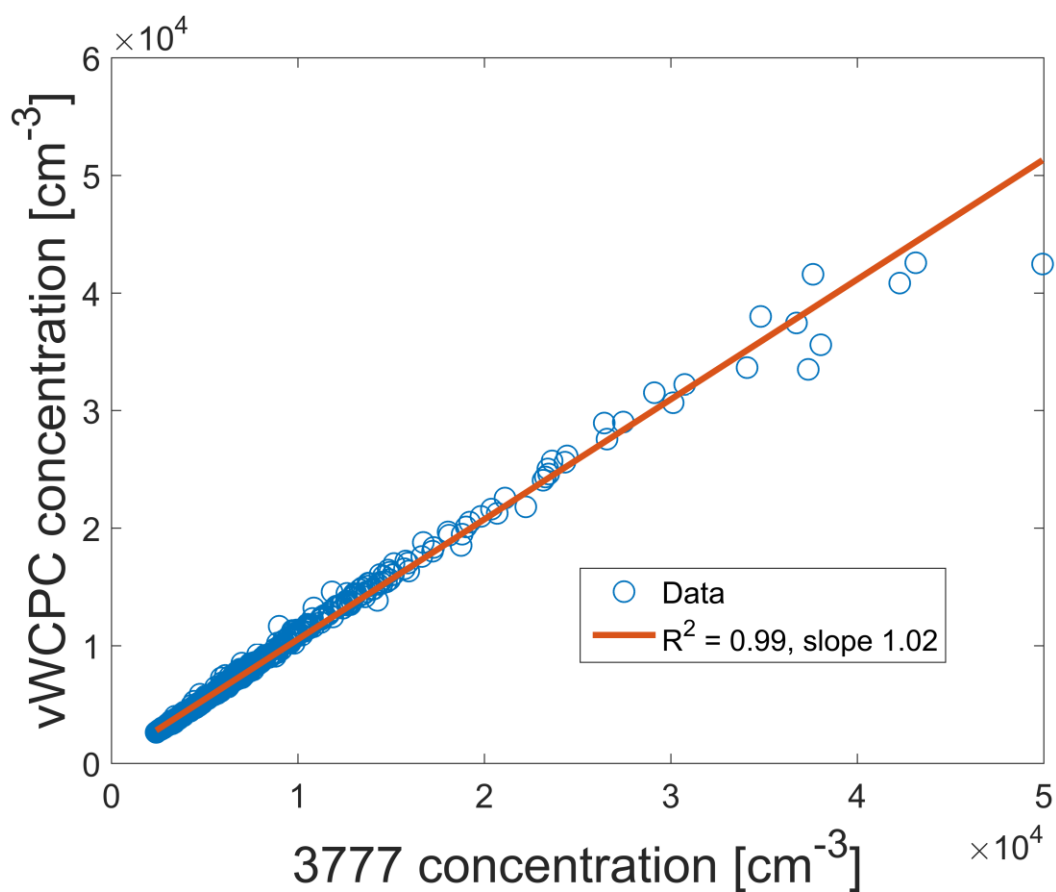
551
552 Figure 11. Correlation of the concentrations below 50 000 cm^{-3} measured by the CPCs for the same
553 data as in Figure 10.
554
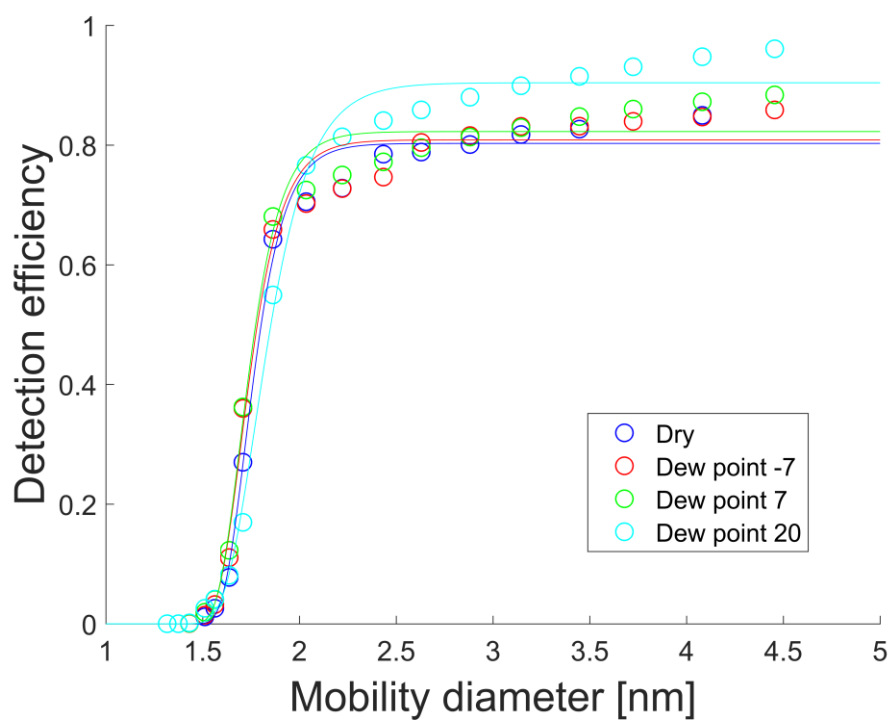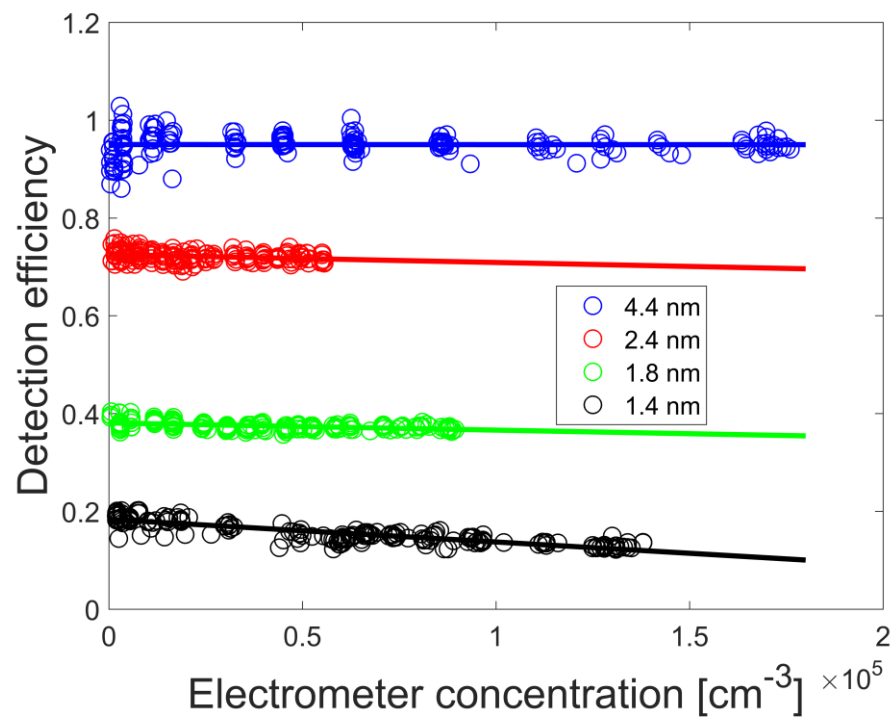
555
556 Figure 12. Detection efficiency of the 3777 as a function of the diameter and sample flow relative
557 humidity.
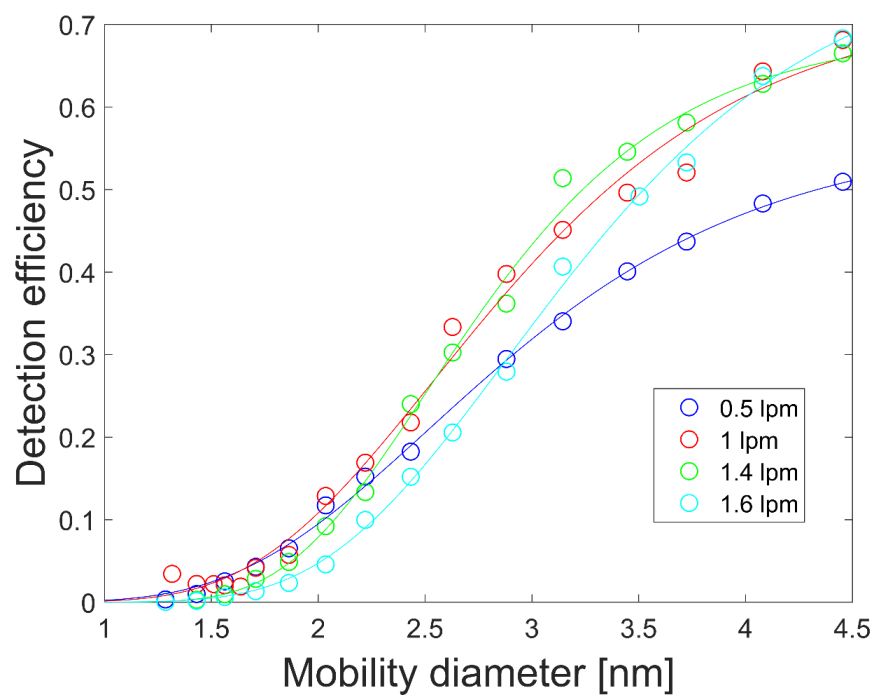
559
560   Figure 13. Detection efficiency of the B3010 as a function of the inlet flow rate.
561

562
563   Figure 14. Ratio of the v-WCPC to the electrometer as function of the particle concentration.
564
565
566   Table 1. Instrument operation conditions

Instrument	Qinlet [lpm]	Qaerosol [lpm]	Settings	Ts [oC]	Tc [oC]	Tm [oC]	To [oC]
B3010	1	1	Low dT	55	10		56

v-WCPC	2.2	0.3	Low dT	8	90	22	40
v-WCPC	2.2	0.3	High dT	1	95	22	40
3777	2.5	0.15	Low dT	62	12		
3777	2.5	0.15	High dT	70	7		

Table 2. Indicated Cutpoints

Conditions	Aerosol	Charging state	ADI v-WCPC	TSI-3777	B3010
High dT	WOx	negative	1.4	1.3	NA
High dT	WOx	positive	1.5	1.4	NA
High dT	WOx	neutral from -	1.6	1.5	NA
High dT	WOx	neutral from +	2.2	2.1	NA
Low dT	WOx	negative	1.7	1.8	3.4
Low dT	WOx	positive	1.9	2	3.2
Low dT	WOx	neutral from -	2	1.9	NA
Low dT	WOx	neutral from +	2.4	2.3	NA
High dT	TDDAB	positive	2.8	NA	NA
Low dT	TDDAB	positive	3.3	2.5	NA